Power System Technology
ISSN:1000-3673

Received: 16-04-2025 Revised: 05-05-2025 Accepted: 22-07-2025

Effects of Slip Conditions on Unsteady MHD Flow of Viscoelastic Fluids in a Porous Channel with Heat and Mass Transfer

B.Sridevi[1], U.Sujatha[2], S.Sridhar [3] N.Venkatnaidu[4], S.Savitha[5]

[1,24,5] Assistant Professor of Mathematics, Dept.of Humanities and Sciences,
Mail: bsridevi@ashokacollege.in

[3]Assistant Professor, Dept. of Mathematics, Narayana Engineering College, SPSR Nellore, Andhrapradesh India.

Corresponding Author,S.Sridhar:drsridhar.nech25@gmail.com

Abstract:-

This paper investigates the impact of slip conditions on the unsteady magnetohydrodynamic (MHD) flow of incompressible viscoelastic fluids in a porous channel. The study considers the influence of a transverse magnetic field, Hall current, and heat and mass transfer. The channel flow is driven by an oscillatory external pressure gradient. Using a perturbation technique, the governing equations for velocity, temperature, and concentration distributions are solved. The analysis includes results for skin friction, the Nusselt number, and the Sherwood number, with numerical computations of skin friction presented in tabular form. Graphical representations illustrate the effects of key flow parameters on fluid behavior, heat and mass transfer, and skin friction. The results highlight how physical parameters influence the system, and the solutions for Newtonian fluids are retrieved as a special case by setting the viscoelastic parameter to zero.

Keywords: magnetohydrodynamic, velocity, temperature, Nusselt number, Newtonian fluids

1. Introduction

Newtonian fluids, governed by the Navier–Stokes equations, have been extensively explored due to their mathematical simplicity and the ease of obtaining analytical solutions. However, their applicability is often limited in practical scenarios, as many industrial and biological fluids such as blood, polymer solutions, clay coatings, greases, and emulsions do not exhibit Newtonian behavior. These fluids are known as non-Newtonian fluids, and they exhibit complex rheological properties that cannot be captured using classical fluid models. Non-Newtonian fluids are generally classified into three categories based on their response to shear. Among these, differential-type fluids include the second-grade (viscoelastic) fluid, which is recognized as one of the simplest and most analytically tractable models in this class

Power System Technology
ISSN:1000-3673

Received: 16-04-2025 Revised: 05-05-2025 Accepted: 22-07-2025

(1–5). Consequently, the second-grade fluid model has been widely adopted for theoretical investigations, including the present study.

Magnetohydrodynamics (MHD), which deals with the flow of electrically conducting fluids under the influence of a magnetic field, has attracted considerable research interest due to its applications in various engineering and industrial processes. MHD flows are particularly relevant in the operation of power generators, MHD accelerators, and processes such as crude oil purification and in the petroleum industry. In recent years, the study of MHD flow through porous media has gained attention owing to its importance in filtration, insulation, geothermal systems, and other energy-related applications (6–14).

The no-slip boundary condition, typically assumed in classical fluid mechanics, does not always hold true at micro or nanoscale levels. To account for velocity slip at the boundary, Navier (15) proposed a slip condition where the slip velocity is proportional to shear stress at the wall. This concept has been the subject of many rigorous studies that investigate fluid flow behavior under various slip conditions (16–22). Notably, Makinde and Mhone (23) examined unsteady MHD oscillatory free convection flow of a viscous fluid in a porous channel, laying the groundwork for further development in this area. Building upon their work, Mehmood and Ali(24) incorporated velocity slip into the boundary conditions. However, both of these studies contained inaccuracies in the transformation of the second thermal boundary condition, leading to erroneous results.

In an effort to correct these issues, Kumar et al. (25) revisited the problem and applied a perturbation technique, reversing the boundary conditions on the porous channel walls. However, the resulting expressions for velocity and temperature, as provided in their equations (13) and (14), failed to fully satisfy the prescribed boundary conditions. These shortcomings highlighted the need for a more rigorous and accurate treatment of the problem.

Furthermore, the combined study of heat and mass transfer has wide applications in several areas of science and engineering, including chemical processing, cooling of electronic equipment, food preservation, and nuclear reactor systems (26–28). This multidimensional complexity calls for advanced fluid models capable of capturing thermal and solutal effects under electromagnetic influence.

2. Mathematical Formulation of the Problem:

We examine the oscillatory flow of an incompressible viscoelastic fluid within a channel filled with a saturated porous medium. The fluid is assumed to be electrically conducting

Power System Technology
ISSN:1000-3673

Received: 16-04-2025 Revised: 05-05-2025 Accepted: 22-07-2025

under the influence of a uniform magnetic field B0, applied transversely along the positive y-axis. Additionally, the magnetic Reynolds number is considered sufficiently small, allowing the effects of the induced magnetic field to be neglected. These assumptions form the basis of the analysis that the

The external electric field is assumed to be zero, and the electric field resulting from polarization is considered negligible. The analysis incorporates the effects of the Hall current. The upper boundary of the channel is maintained at a constant temperature T_w and concentration level C_w while the ambient fluid has uniform temperature T_0 and concentration C_0. A slip condition is applied at the lower boundary, and the energy equation accounts for the effect of thermal radiation. The x-axis is aligned with the flow direction, and the y-axis is perpendicular to the flow, as illustrated in Fig. 1.Under the standard Boussinesq approximation, the governing equations for momentum, energy, and concentration can be expressed as follows:

$$\rho\frac{\partial u}{\partial t} = -\frac{\partial p}{\partial x} + \mu\frac{\partial^2 u}{\partial y^2} + \alpha_1\frac{\partial^3 u}{\partial y^2 \partial t} + g\beta_{\mathrm{T}}(T - T_0) + g\beta_{\mathrm{C}}(C - C_0) - \frac{\sigma B_0^2(1 + \mathrm{i}m)u}{1 + m^2}$$

subject to the boundary conditions

$$u(0,t) - \eta\left(\frac{\partial u(0,t)}{\partial y} + \frac{\alpha_1}{\mu}\frac{\partial^2 u(0,t)}{\partial y \partial t}\right) = 0,$$
$$T(0,t) = T_0, C(0,t) = C_0,$$

where $u = u(y,t)$ denotes the fluid velocity in the x-direction, $T = T(y,t)$ and $C = C(y,t)$ are the temperature and concentration respectively, ρ is the fluid density, μ is the viscosity, α_1 is the viscoelastic or second grade parameter, σ is the electrical conductivity of the fluid, m is the Hall parameter, β_{T} is the volumetric coefficient of thermal expansion, β_{C} is the volumetric coefficient of concentration expansion, g is the acceleration due to gravity, $\phi_1 (0 < \phi_1 < 1)$ and $k_1 > 0$ are the porosity and permeability of the porous medium respectively, c_p is the specific heat capacity, k is the thermal conductivity, q_{r} is the radiative heat flux in y-direction, D is the mass diffusivity, T_{m} is the mean fluid temperature, K_{T} the thermal-diffusion ratio, η is the slip parameter, and a is the width of the channel.

Power System Technology
ISSN:1000-3673

Received: 16-04-2025 Revised: 05-05-2025 Accepted: 22-07-2025

For oscillatory flow, we take the external pressure gradient of the form $(\partial p/\partial x) = -\lambda e^{i\omega t}$, where λ is constant and ω is the frequency of oscillation. Further, we assume that the temperature of the plates T_0 and T_w are high enough to produce the radiative heat transfer and following Cogley et al., [29] the radiative heat flux is given by [23]

$$-\frac{\partial q_r}{\partial y} = 4\alpha_0^2(T - T_0) \tag{5}$$

where α_0 is the mean radiation absorption coefficient.
By keeping in mind the above assumptions and introducing the following dimensionless variables

$$x^* = ax, y^* = ay, u^* = U_0 u, t^* = \frac{at}{U_0},$$

the system of eqs. (1)-(4) reduces to (* notations are dropped for the sake of simplicity)

$$a_1\frac{\partial u}{\partial t} - \frac{\partial^2 u}{\partial y^2} - \alpha\frac{\partial^3 u}{\partial y^2 \partial t} + Hu - Gr\theta - Gm\phi = \lambda e^{i\omega t},$$
$$u(0,t) - \eta\left(\frac{\partial u(0,t)}{\partial y} + \alpha\frac{\partial^2 u(0,t)}{\partial y \partial t}\right) = 0$$
$$Pe\frac{\partial \theta}{\partial t} = \frac{\partial^2 \theta}{\partial y^2} + N^2\theta$$
$$\frac{1}{Sc}\frac{\partial \phi}{\partial t} = \frac{\partial^2 \phi}{\partial y^2} + Sr\frac{\partial^2 \theta}{\partial y^2},$$

where

$$\mathrm{Re} = \frac{aU_0}{\nu}, \alpha = \frac{\alpha_1 U_0}{\mu a}, M^2 = \frac{\sigma B_0^2 a^2}{\mu}$$

Power System Technology
ISSN:1000-3673

Received: 16-04-2025 Revised: 05-05-2025 Accepted: 22-07-2025

$$\frac{1}{K}=\frac{a^2\phi_1}{k_1}, Sc=\frac{D}{aU_0}, a_1=Re+\frac{\alpha}{k_1},$$
$$N^2=\frac{4a^2\alpha_0^2}{k}, Gr=\frac{g\beta_{\mathrm{T}}a^2(T_{\mathrm{w}}-T_0)}{\mu U_0},$$
$$Gm=\frac{g\beta_{\mathrm{C}}a^2(C_{\mathrm{w}}-C_0)}{\mu U_0}, \eta^*=\frac{\eta}{a},$$
$$H=\frac{M^2(1+\mathrm{i}m)}{1+m^2}+\frac{1}{K}, Sr=\frac{DK_{\mathrm{T}}(T_{\mathrm{w}}-T_0)}{DT_{\mathrm{m}}(C_{\mathrm{w}}-C_0)},$$

Here α is the dimensionless viscoelastic parameter, M is the magnetic parameter called Hartmann number, K is the permeability parameter, η (* notation is dropped) is the dimensionless slip parameter, Re is the Reynold's number, N is the radiation parameter, Pe is the Peclet number, Gr is the thermal Grashof number, Gm is the mass Grashof number, Sc is the Schmidt number, and Sr is the Soret number.

3. Solution of the Problem:

Owing to the pressure gradient of oscillatory form and in order to solve eqs. (7)-(9), we are looking for the following perturbation solutions:

$$u(y,t)=u_0(y)+\epsilon \mathrm{e}^{\mathrm{i}\omega t}u_1(y)+O(\epsilon^2),$$
$$\theta(y,t)=\theta_0(y)+\epsilon \mathrm{e}^{\mathrm{i}\omega t}\theta_1(y)+O(\epsilon^2),$$

where $u(y,t), \theta(y,t)$, and $\phi(y,t)$ are the dimensionless velocity, temperature and concentration fields.

Using eq. (11) into eqs. (7)-(9), we obtain the following system of ordinary differential equations.

Power System Technology
ISSN:1000-3673

Received: 16-04-2025 Revised: 05-05-2025 Accepted: 22-07-2025

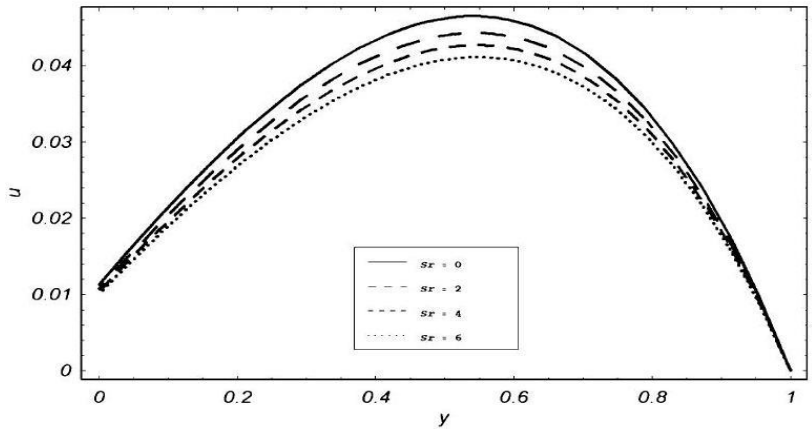

$$\frac{\mathrm{d}^2u_0(y)}{\mathrm{d}y^2} - m_1^2u_0(y) = -Gr\theta_0(y) - Gm\phi_0(y) \tag{12}$$

$$u_0(0) - \eta\frac{\mathrm{d}u_0(0)}{\mathrm{d}y} = 0, u_0(1) = 0, \tag{13}$$

$$\frac{\mathrm{d}^2u_1}{\mathrm{d}y^2} - m_2^2u_1(y) = -\lambda_0, \tag{14}$$

$$u_1(0) - \gamma\frac{\mathrm{d}u_1(0)}{\mathrm{d}y} = 0, u_1(1) = 0, \tag{15}$$

$$\frac{\mathrm{d}^2\theta_0(y)}{\mathrm{d}y^2} + N^2\theta_0(y) = 0; \theta_0(0) = 0, \theta_0(1) = 1, \tag{16}$$

$$\frac{\mathrm{d}^2\theta_1(y)}{\mathrm{d}y^2} + (N^2 - \mathrm{i}\omega Pe)\theta_1(y) = 0 \tag{16}$$

$$\theta_1(0) = 0, \theta_1(1) = 0 \tag{17}$$

$$\frac{\mathrm{d}^2\phi_0(y)}{\mathrm{d}y^2} + Sr\frac{\mathrm{d}^2\theta_0(y)}{\mathrm{d}y^2} = 0; \phi_0(0) = 0, \phi_0(1) = 1, \tag{18}$$

$$\frac{\mathrm{d}^2\phi_1(y)}{\mathrm{d}y^2} - \mathrm{i}wSc\phi_1(y) = -Sr\frac{\mathrm{d}^2\theta_1(y)}{\mathrm{d}y^2}; \tag{18}$$

$$\phi_1(0) = 0, \phi_1(1) = 0 \tag{19}$$

where

$$\gamma = \eta(1 + \mathrm{i}\alpha\omega), \lambda_0 = \frac{\lambda}{\epsilon(1 + \mathrm{i}\alpha\omega)}$$

The solutions of eqs. (16)-(19) yield

Power System Technology
ISSN:1000-3673

Received: 16-04-2025 Revised: 05-05-2025 Accepted: 22-07-2025

$$\theta_1(y) = 0, \phi_1(y) = 0 \quad (21)$$

$$\theta_0(y) = a_2 \sin(Ny), \phi_0(y) = -a_2 \mathrm{Sr} \sin(Ny) + a_3 y. \quad (22)$$

Using eq. (22) into eq. (12), we get

$$u_0(y) = c_1 \cosh(m_1) y + c_2 \sinh(m_1) y$$

Where

$$a_3 = (1 + Sr), a_4 = a_2 GmSr - a_2 Gr,$$
$$a_2 = \frac{1}{\sin N}, a_6 = \frac{a_4}{N^2 + m_1^2}, a_7 = \frac{a_5}{m_1^2},$$
$$c_1 = \eta m_1 c_2 - \eta a_6 N + \eta a_7, a_5 = a_3 Gm$$
$$c_2 = \frac{\eta(a_6 N - a_7)\cosh m_1 + a_6 \sin N - a7}{\eta m_1 \cosh m_1 + \sinh m_1},$$
$$c_3 = -\frac{\lambda_0}{m_2^2} + \frac{\gamma \lambda_0 [\cosh(m_2) - 1]}{m_2 [\gamma m_2 \cosh(m_2) + \sinh(m_2)]},$$

Now substituting eqs. (21)-(24) into eq. (11), we arrive at the following solutions

$$\theta(y,t) = a_2 \sin(Ny), \quad (26)$$

$$\phi(y,t) = -a_2 \mathrm{Sr} \sin(Ny) + a_3 y, \quad (27)$$

$$u(y,t) = c_1 \cosh(m_1) y + c_2 \sinh(m_1) y - a_6 \sin(Ny) + a_7 y \quad (27)$$

$$+\epsilon e^{i\omega t} \left[c_3 \cosh(m_2) y + c_4 \sinh(m_2) y + \frac{\lambda_0}{m_2^2} \right] \quad (28)$$

Furthermore, it is found from the eq. (28) that the corresponding solutions for Newtonian fluid can be obtained as a limiting case by taking the viscoelastic parameter α equal to zero. Similarly, the solutions for a hydrodynamic viscoelastic fluid passing through a non-porous medium and those for the no slip condition can also be obtained as limiting cases. Furthermore, the above solutions (26)-(28), also satisfy the imposed boundary conditions which provides a useful mathematical check.

Skin-friction: We evaluate the expression of skin-friction from eq. (28) as:

$$\tau = \tau(t)$$
$$= a_7 + c_2 m_1 - a_6 N$$

Nusselt number: We evaluate the rate of heat transfer from eq. (26) as:

$$Nu = \frac{N}{\sin N} \quad (30)$$

Sherwood number: We evaluate the rate of mass transfer from eq. (27) as:

Power System Technology
ISSN:1000-3673

Received: 16-04-2025 Revised: 05-05-2025 Accepted: 22-07-2025

$$Sh = -\frac{\mathrm{Sr}N}{\sin(N)} + (1 + Sr) \tag{31}$$

4. Graphical Results and Discussion

This section deals with the effect of various pertinent parameters on velocity, temperature and concentration profiles. The parameters entering into the fluid flow are

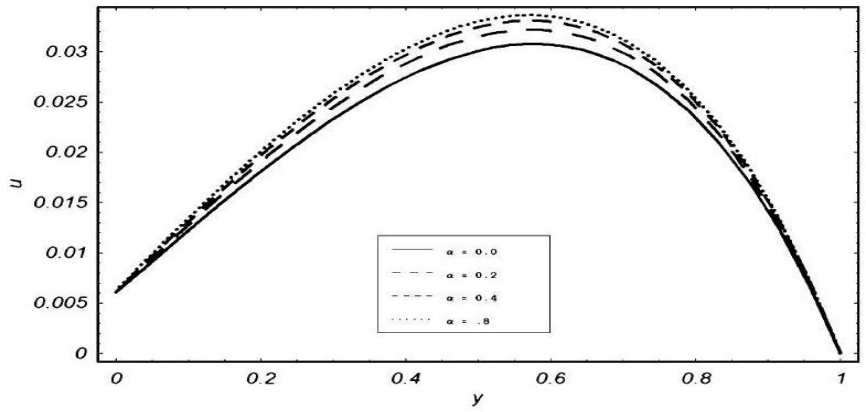

Fig. 1. Velocity profiles for different values of α when $\omega t = \pi/2, Re = 1,\ Gr = 0.1, M = 0.5, K = 1.5,\quad Gm = 0.5, Sr = 2.0, N = 0.2, \omega = 0.1,\quad \eta = 0.1, \lambda = 0.1, m = 0.1, \epsilon = 0.1.$ viscoelastic parameter α, magnetic parameter M, permeability parameter K, thermal Grashof number Gr, Soret number Sr, radiation parameter N, slip parameter η, phase angle ωt, Hall parameter m, and mass Grashof number Gm. For this purpose, Figs. 2-14 are sketched. In these figures, Figs. 1-11 are plotted to show the effects of $\alpha, M, K, Gr, Sr,\ N, \eta, \omega t, m$, and Gm on velocity, Figs. 11-13 are sketched to show the effects of Sr and N on the temperature and concentration of the fluid respectively.

The effect of viscoelastic parameter α on the flow of a second grade fluid is shown in Fig. 2. From this figure, it is clear that the velocity of the fluid strongly depends on the viscoelastic parameterα. We found that the velocity and boundary layer thickness increase in the middle of the channel as α increases. However, the variation in velocity is relatively insignificant near the boundaries of the channel. The effects of viscoelastic parameter α are weaker near the boundary at $y = 0$, and increase with increasing distance from the boundary, ultimately the velocity approaches its maximum value where it again starts the decline motion tending to the minimum value at the boundary $y = 1$. Such a behavior of velocity for the viscoelastic parameter α is quite identical to the already published work in the literature (see, for

Power System Technology
ISSN:1000-3673

Received: 16-04-2025 Revised: 05-05-2025 Accepted: 22-07-2025

example, Figs. 3, 7, and 11 in ref. 11). Furthermore, this figure also shows the comparison of velocity for Newtonian and second grade fluids. It is observed that velocity of the Newtonian fluid ($\alpha = 0$), is smaller in magnitude compare to the second grade fluid. Physically, it is true in the sense that the second grade fluid can move fast due to the elastic properties of the fluid which are absent in case of Newtonian fluid.

The effect of the magnetic field on the flow pattern is shown in Fig. 3. A comparative study of the MHD flow and non-MHD flow reflects that the velocity of the hydrodynamic second grade fluid is greater than the magneto hydrodynamic second grade fluid. The curve with $M = 0$ corresponds to the case of non-MHD flow. The effect of the magnetic parameter M is to decrease the velocity of the fluid. The higher this value the prominent is the reduction in the velocity. This physical interpretation of the velocity is an indication that the increasing values of magnetic parameter M generate the resistive type force also called Lorentz force, which acts in the opposite direction of the fluid motion and

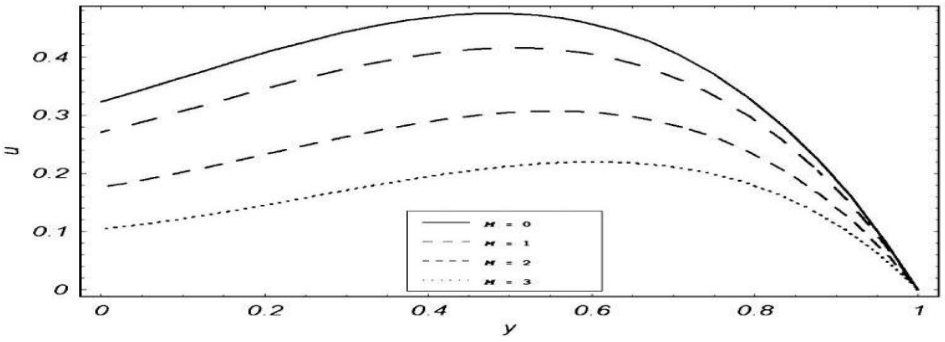

Fig. 2. Velocity profiles for different values of M when $\omega t = 0, Re = 1, Gr = 5, K = 0.5, \alpha = 0.5, Gm = 1.5, Sr = 2.0, N = 0.2, \omega = 0.1, \eta = 0.8, \lambda = 0.1, m = 0.1, \epsilon = 0.1$.

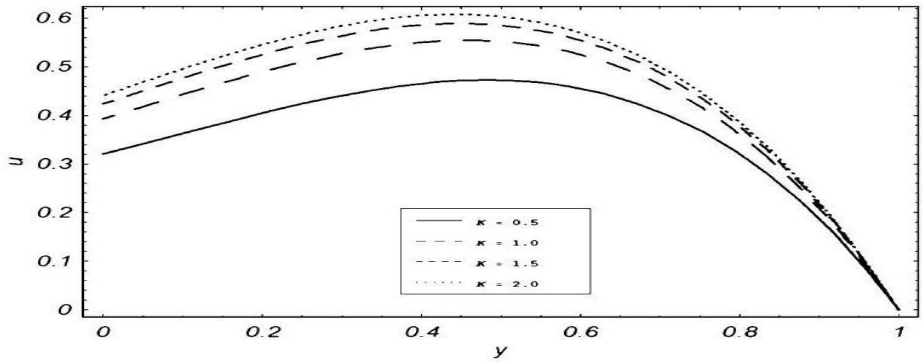

Fig. 3. Velocity profiles for different values of K when $\omega t = 0, Re = 1, Gr = 5, M = 0.2, Gm = 1.5, \alpha = 0.5, Sr = 2.0, N = 0.2, \omega = 0.1, \eta = 0.1, \lambda = 0.1, m =$

Power System Technology
ISSN:1000-3673

Received: 16-04-2025 Revised: 05-05-2025 Accepted: 22-07-2025

$0.1, \epsilon = 0.1$.
tends to resist the flow thereby reducing the velocity. Furthermore, it is noticed that increasing the transverse magnetic field, therefore act to thin the boundary layer thickness.

Figure 3 is plotted to show the effect of permeability parameter K of the porous medium on the velocity. It appears from this figure that as we increase the permeability of the porous medium, it reduces the drag force and causes the velocity profiles to increase. Thus, the increasing values of the permeability parameter K of the porous medium yields an effect opposite to that of the magnetic parameter M . This physical behavior is in accordance with the mathematical relation of M and K as given in eqs. (7) and (10).

The velocity profiles for different values of thermal Grashof number Gr is presented in Fig. 5. It is observed that an increase in thermal Grashof number Gr, leads to increase velocity due to enhancement in buoyancy force. Actually, thermal Grashof number signifies the relative effect of the thermal buoyancy force to the viscous hydrodynamic force. Increase of Grashof number Gr means an increase of temperature gradients due to which the contribution from the buoyancy near the plate becomes significant and hence a short rise in the velocity near the plate is observed. Physically $Gr < 0$, means cooling of thefluidorheating

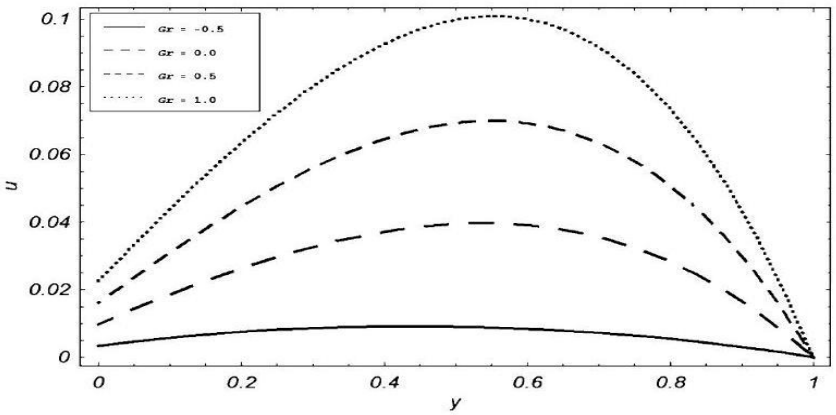

Fig. 4. Velocity profiles for different values of Gr when $\omega t = 0, Re = 1, M = 0.7, K = 1, Gm = 0.5, \alpha = 0.5, Sr = 0.8, N = 0.5, \omega = 0.8, \eta = 0.1, \lambda = 0.1, m = 0.1, \epsilon = 0.1$.

Power System Technology
ISSN:1000-3673

Received: 16-04-2025 Revised: 05-05-2025 Accepted: 22-07-2025

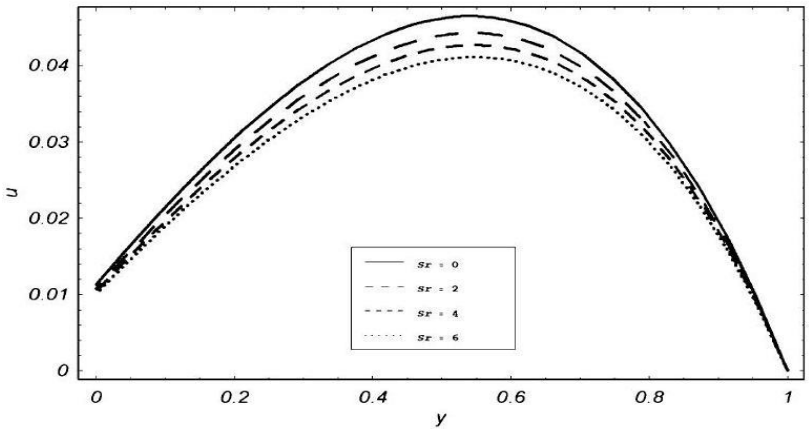

Fig. 5. Velocity profiles for different values of Sr when $\omega t = 0, Re = 1,\ Gr = 0.1, M = 0.7, K = 1, Gm = 0.5, \alpha = 0.5, N = 0.5, \omega = 0.1, \eta = 0.8, \lambda = 0.1, m = 0.1, \epsilon = 0.1$.

of the plate, $Gr = 0$ corresponds to the absence of free convection current and $Gr > 0$ means heating of the fluid or cooling of the plate by natural convection. For the positive value of Gr, heat is conducted away from the boundary into the fluid which increases the temperature and thereby enhances the buoyancy force.

Figure 5 illustrates variations in velocity for different values of Soret number Sr . It is found that velocity decreases for large values of Sr. The effect of Soret number on velocity is identical to that of magnetic parameter. However, the variations in the boundary layer thickness for Soret number Sr are smaller compare to the magnetic parameter M.The effect of radiation parameter N on the velocity is illustrated in Fig. 7. It is seen that an increase in the radiation parameter contributes to the decrease in the velocity field. It means that the velocity decreases in the presence of high thermal radiation. Furthermore, it is observed that in the absence of radiation $(N \to 0)$ which physically corresponds to high thermal conductivity $(k \to \infty)$, the velocity of the fluid is maximum and decreases for further increasing values of N.

The velocity versus y graph for different values of slip parameter η is shown in Fig. 8. It is depicted from this figure that velocity increases when the slip parameter η is increased. Physically, this is possible due to the fact that as we increase the slip parameter, the force which keeps in

Power System Technology
ISSN:1000-3673

Received: 16-04-2025 Revised: 05-05-2025 Accepted: 22-07-2025

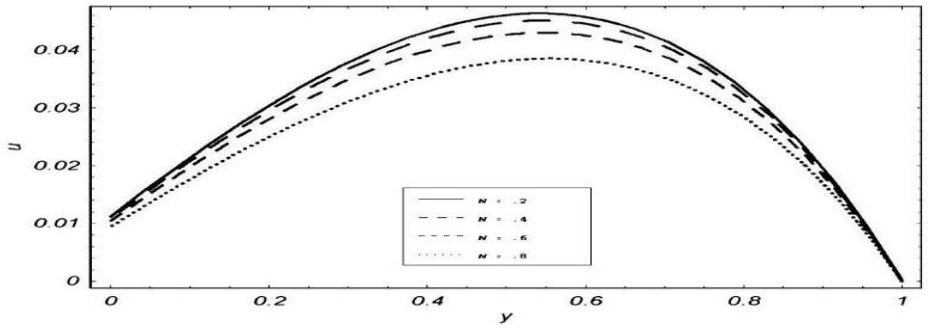

Fig. 6. Velocity profiles for different values of N when $\omega t = 0, Re = 1,\ Gr = 0.1, M = 0.7, K = 1, Gm = 0.5, \alpha = 0.5, Sr = 1, \omega = 0.8, \eta = 0.1, \lambda = 0.1, m = 0.1, \epsilon = 0.1$.

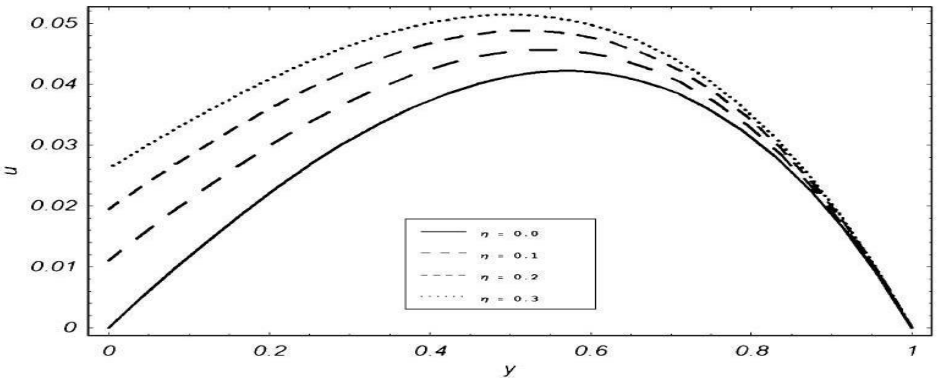

Fig. 7. Velocity profiles for different values of η when $\omega t = 0, Re = 1,\ Gr = 0.1, M = 0.7, K = 1, Gm = 0.5, \alpha = 0.5, Sr = 1, N = 0.2, \omega = 0.8, \lambda = 0.1, m = 0.1, \epsilon = 0.1$.

contact the fluid and the plate together, decreases and therefore; the fluid can move fast. Furthermore, we can see from this figure that for the case of no slip condition ($\eta = 0$), velocity of the second grade fluid is zero at both of the boundaries. However, for further increasing values of η, velocity increases. A similar effect of the slip parameter η on the velocity was expected in view of the boundary conditions of velocity in eq. (7). These graphical results of velocity for different η are in accordance with already published work by Mehmood and Ali[24] (Fig. 1) and Khan et al. [27] (Fig. 2).

The graphical results for the phase angle ωt are displayed in Fig. 8. It is found that velocity decreases for large values of ωt when the thermal Grashof number $Gr = 0.1$, which physically corresponds to the cooling of the plate. Further, it is noted that the velocity starts to increase near the plate, reaches a maximum value and then starts to decay and finally approaches to zero. The effects of Hall parameter m on the velocity profile is shown in Fig. 9. It is depicted from this figure that velocity increases with an increase in the values of m. A

Power System Technology
ISSN:1000-3673

Received: 16-04-2025 Revised: 05-05-2025 Accepted: 22-07-2025

similar behavior of m is also expected due to the fact that the Hall parameter is inversely proportional to the magnetic parameter M as shown in eq. (1), which reduce the Lorentz force and consequently the velocity increases. Furthermore, the velocity profiles for various values of the mass Grashof number Gm are shown in

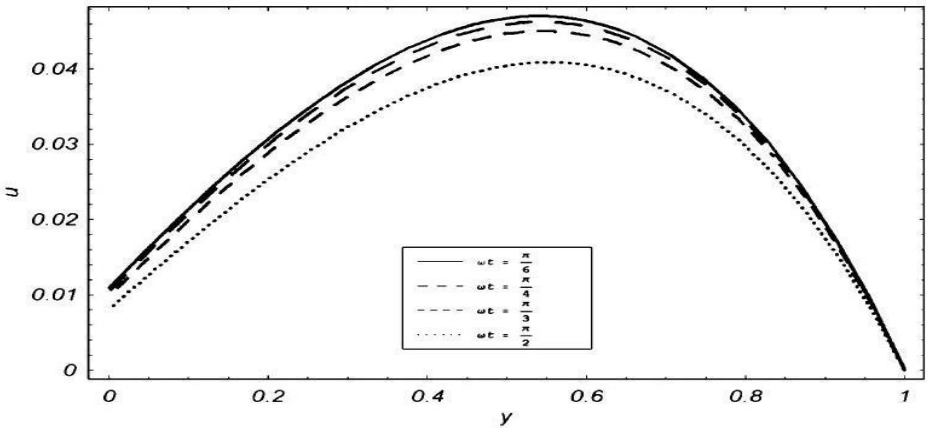

Fig. 8. Velocity profiles for different values of ωt when $= 1, Gr = 0.1, M = 0.7, K = 1, Gm = 0.5, \alpha = 0.5, Sr = 1, N = 0.2, \omega = 0.8, \eta = 0.1, \lambda = 0.1, m = 0.1, \epsilon = 0.1$.

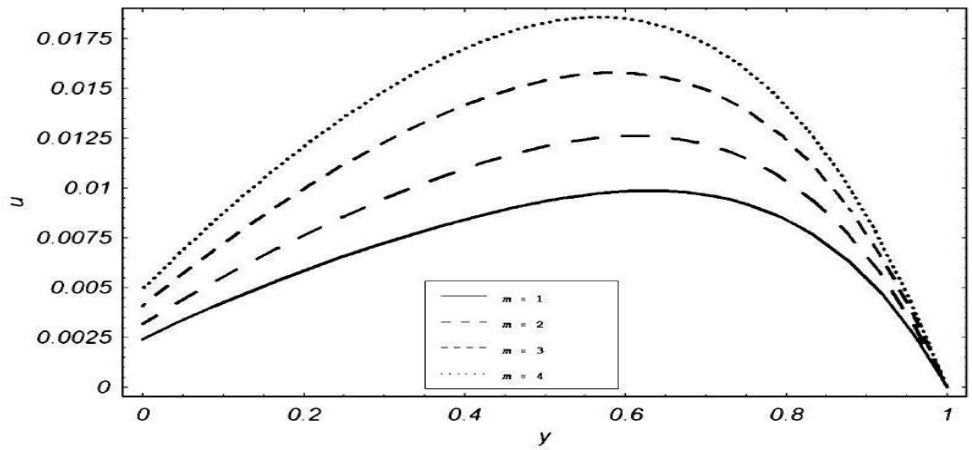

Fig. 9. The velocity profiles for different values of m when $\omega t = 0$, $Re = 1, Gr = 0.1, M = 5, K = 2, Gm = 0.2, \alpha = 0.5, Sr = 0.5, N = 0.7, \omega = 0.8, \eta = 0.1, \lambda = 0.1, \epsilon = 0.1$.

Power System Technology
ISSN:1000-3673

Received: 16-04-2025 Revised: 05-05-2025 Accepted: 22-07-2025

Fig. 10. It is interesting to note that $Gm = 0$, corresponds to the absence of free convection current or buoyancy force whereas $Gm > 0$ corresponds to a strong magnetic field and to a cooling problem that is generally encountered in nuclear engineering in connection with the cooling of the reactor. It is clear from this figure that for large values of Gm, the buoyancy force increases and consequently accelerates the flow.

The graphical results of temperatureθ, and concentration ϕ for different values of radiation parameter N are shown in Figs. 11 and 12. It is found from Fig. 11, that temperature increases as thermal radiation parameter N increases. Physically, this is in agreement with the fact that the thermal boundary layer thickness increases with increasing values of the radiation parameter$N$. However; the concentration profiles show opposite behavior compare to temperature profiles for the increasing values of the radiation parameter N. This fact is shown in Fig. 12. The influence of Soret number Sr on the concentration profile is shown in Fig. 14. As the Soret number is related to the mass transfer of the flow, therefore, the concentration profiles show a large amount of variation and increase significantly when Soret number is increased.The numerical results for the skin friction are shown in Table I. The effects of various embedded parameters on the skin friction are studied. It is found that the skin friction

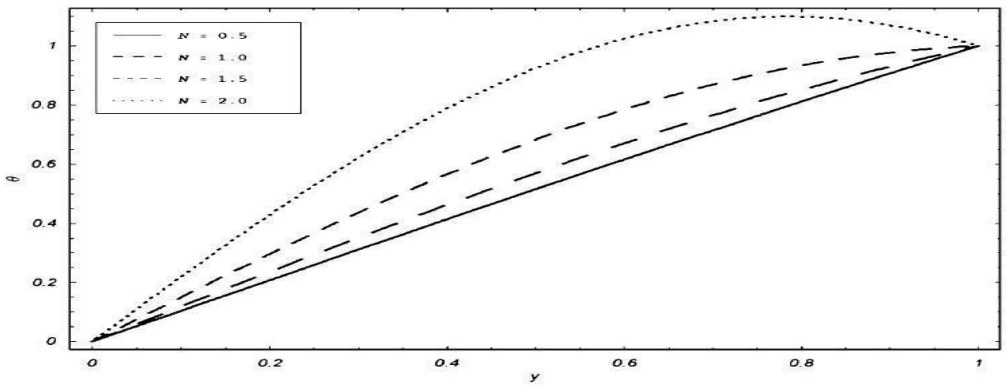

Fig. 11. Velocity profiles for different values of G_m when $\omega t = 0$, Re $= 1, Gr = 5, M = 0.7, K = 0.5, \alpha = 0.5, Sr = 2, N = 0.2, \omega = 0.1, \eta = 0.8, \lambda = 0.1, m = 0.1, \epsilon = 0.1$.

Power System Technology
ISSN:1000-3673

Received: 16-04-2025 Revised: 05-05-2025 Accepted: 22-07-2025

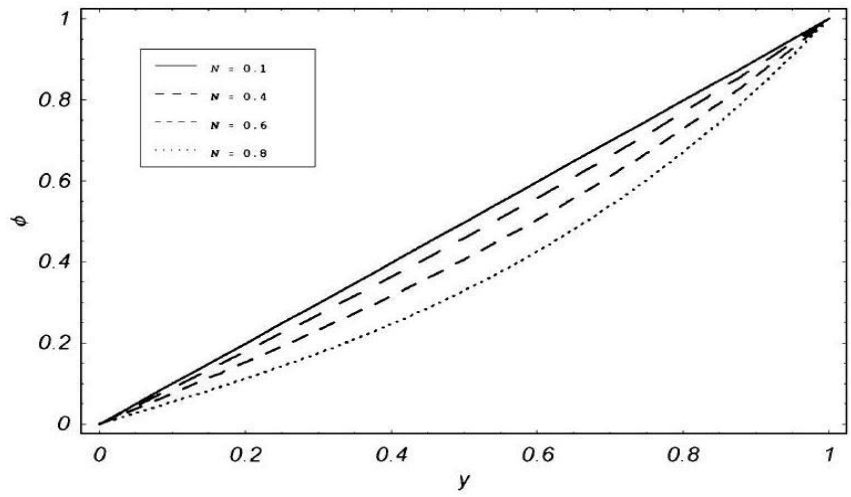

Fig. 12. Concentration profiles for different values of N when $Sr = 4$.

decreases when the viscoelastic parameter α is increased. The results for the magnetic parameter M, the permeability parameter K and the Hall current m have the similar effects on the skin friction as reported by Agrawal et al. [13] The skin friction decreases when M is increased while increases for the increasing values of K and m. Furthermore, it is clear from this table that for the increasing values of both Grashof number Gr and wall slip parameter η, the skin friction decreases. It is due to the fact when Gr and η are increased, they undermine the resistance force and consequently reduces the skin friction. Also, Table I shows that the skin

Table I. The effect of various parameters on the skin friction.

	ωt	Re	Gr	M	K	Gm	α	Sr	N	ω	η	λ	m	ϵ	τ
$\alpha = 0.2$	0	1	0.5	0.7	2	1.5	0.2	2	2	0.8	0.1	0.1	0.1	0.1	5.111
$\alpha = 0.4$	0	1	0.5	0.7	2	1.5	0.4	2	2	0.8	0.1	0.1	0.1	0.1	4.999
$\alpha = 0.6$	0	1	0.5	0.7	2	1.5	0.6	2	2	0.8	0.1	0.1	0.1	0.1	4.884

Power System Technology
ISSN:1000-3673

Received: 16-04-2025 Revised: 05-05-2025 Accepted: 22-07-2025

$M = 0$	0	1	0.5	0	2	1.5	0.2	2	2	0.8	0.1	0.1	0.1	0.1	3.93
$M = 1$	0	1	0.5	1	2	1.5	0.2	2	2	0.8	0.1	0.1	0.1	0.1	3.88
$M = 2$	0	1	0.5	2	2	1.5	0.2	2	2	0.8	0.1	0.1	0.1	0.1	3.68
$Gr = -0.5$	0	1	-0.5	0.7	2	1.5	0.2	2	2	0.8	0.1	0.1	0.1	0.1	4.24
$Gr = 0$	0	1	0	0.7	2	1.5	0.2	2	2	0.8	0.1	0.1	0.1	0.1	4.08
$Gr = 0.5$	0	1	0.5	0.7	2	1.5	0.2	2	2	0.8	0.1	0.1	0.1	0.1	3.91
K = 1	0	1	0.5	0.7	1	1.5	0.2	2	2	0.8	0.1	0.1	0.1	0.1	0.032
$K = 2$	0	1	0.5	0.7	2	1.5	0.2	2	2	0.8	0.1	0.1	0.1	0.1	0.035
K = 3	0	1	0.5	0.7	3	1.5	0.2	2	2	0.8	0.1	0.1	0.1	0.1	0.036
$\eta = 0$	0	1	0.5	0.7	2	1.5	0.2	2	2	0.8	0	0.1	0.1	0.1	0.040
$\eta = 1$	0	1	0.5	0.7	2	1.5	0.2	2	2	0.8	1	0.1	0.1	0.1	0.016

Power System Technology
ISSN:1000-3673

Received: 16-04-2025 Revised: 05-05-2025 Accepted: 22-07-2025

$\eta = 2$	0	1	0.5	0.7	3	1.5	0.2	2	2	0.8	2	0.1	0.1	0.1	0.009
$\omega t = \frac{\pi}{6}$	$\frac{\pi}{6}$	1	0.5	0.7	2	1.5	0.2	2	2	0.8	0.1	0.1	0.1	0.1	0.035
$\omega t = \frac{\pi}{4}$	$\frac{\pi}{4}$	1	0.5	0.7	2	1.5	0.2	2	2	0.8	0.1	0.1	0.1	0.1	0.031
$\omega t = \frac{\pi}{2}$	$\frac{\pi}{2}$	1	0.5	0.7	2	1.5	0.2	2	2	0.8	0.1	0.1	0.1	0.1	0.006
$Sr = 0$	0	1	0.5	0.7	2	1.5	0.2	0	2	0.8	0.1	0.1	0.1	0.1	0.356
$Sr = 2$	0	1	0.5	0.7	2	1.5	0.2	2	2	0.8	0.1	0.1	0.1	0.1	0.195
$Sr = 4$	0	1	0.5	0.7	2	1.5	0.2	4	2	0.8	0.1	0.1	0.1	0.1	0.035
$N = 0.2$	0	1	0.5	0.7	2	1.5	0.2	2	0.2	0.8	0.1	0.1	0.1	0.1	0.301
$N = 0.4$	0	1	0.5	0.7	2	1.5	0.2	2	0.4	0.8	0.1	0.1	0.1	0.1	0.296
$N = 0.6$	0	1	0.5	0.7	2	1.5	0.2	2	0.6	0.8	0.1	0.1	0.1	0.1	0.288
$G_m = 0$	0	1	0.5	0.7	2	0	0.2	2	2	0.8	0.1	0.1	0.1	0.1	0.158

Power System Technology
ISSN:1000-3673

Received: 16-04-2025 Revised: 05-05-2025 Accepted: 22-07-2025

$G_m = 1$	0	1	0.5	0.7	2	1	0.2	2	2	0.8	0.1	0.1	0.1	0.1	0.076
$G_m = 1.5$	0	1	0.5	0.7	2	1.5	0.2	2	2	0.8	0.1	0.1	0.1	0.1	0.035
$m = 1$	0	1	0.5	0.7	2	1.5	0.2	2	2	0.8	0.1	0.1	1	0.1	0.036
$m = 2$	0	1	0.5	0.7	2	1.5	0.2	2	2	0.8	0.1	0.1	2	0.1	0.037
$m = 3$	0	1	0.5	0.7	2	1.5	0.2	2	2	0.8	0.1	0.1	3	0.1	0.038

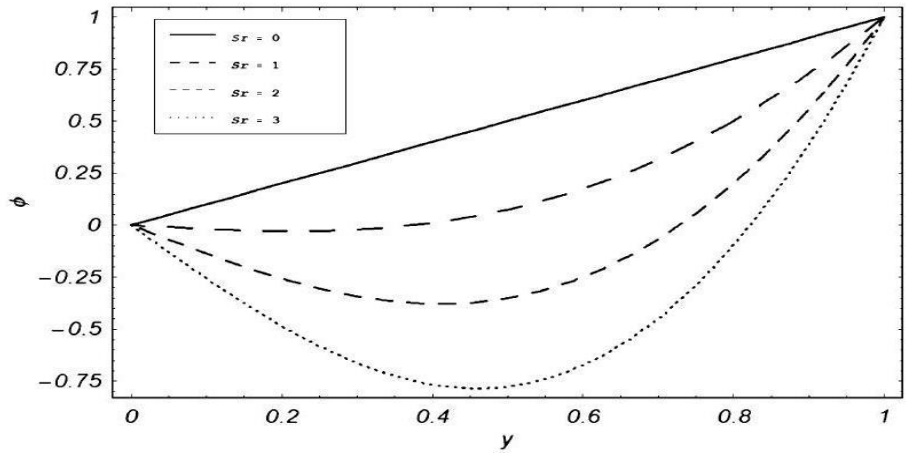

Fig. 13. Concentration profiles for different values of Sr when $N = 2$. friction decreases with the increasing values of phase angle ωt, radiation parameter N, Soret number Sr , and mass Grashof number Gm.

5. Conclusions

In this paper, we analyzed the impact of slip condition on the unsteady MHD flow of viscoelastic fluids passing through a porous channel with heat and mass transfer phenomenon. The flow in the fluid is generated due to the oscillatory pressure gradient.

Power System Technology
ISSN:1000-3673

Received: 16-04-2025 Revised: 05-05-2025 Accepted: 22-07-2025

Using perturbation technique, the solutions for velocity, temperature and concentration are obtained. The corresponding expressions for skin-friction, Nusselt number and Sherwood number are also evaluated. The effects of various parameters on the skin friction are studied numerically. Further, the analytical results are displayed graphically and discussed. The following conclusions are extracted from this study.

1. The increasing values of second grade parameter α increases the fluid velocity and decrease the skin friction.
2. The effects of Hall parameter m on velocity and skin friction are similar to permeability parameter K.
3. Velocity and skin friction decrease for large values of $M, N, \omega t$, and Sr.
4. Velocity increases whereas skin friction decreases when Gr, η, and Gm are increased.
5. The radiation parameter has an opposite effect on θ and ϕ.
6. With increasing values of Sr, ϕ increases.

6. References

1) N. Aksel: Acta Mech. 157 (2002) 235.
2) C. Fetecau and J. Zierep: Acta Mech. 150 (2001) 135.
3) M. E. Erdog˘an and C. E. I˙mrak: Appl. Math. Modelling 31 (2007) 170.
4) C. Fetecau, T. Hayat, C. Fetecau, and N. Ali: Nonlinear Anal.—RealWorld Appl. 9 (2008) 1236.
5) M. Nazar, C. Fetecau, D. Vieru, and C. Fetecau: Nonlinear Anal.—
Real World Appl. 11 (2010) 584.
6) W. C. Tan and T. Masuoka: Int. J. Non-Linear Mech. 40 (2005) 515.
7) T. Hayat, I. Khan, R. Ellahi, and C. Fetecau: J. Porous Media 11
(2008) 389.
8) M. Hussain, T. Hayat, S. Asghar, and C. Fetecau: Nonlinear Anal.—Real World Appl. 11 (2010) 2403.
9) F. Ali, M. Norzieha, S. Sharidan, I. Khan, and T. Hayat: Int. J. Non-Linear Mech. 47 (2012) 521.
10) A. K. Tiwari and S. K. Ravi: Adv. Theor. Appl. Mech. 2 (2009) 33.
11) M. Khan, K. Iqbal, and M. Azram: Spec. Top. Rev. Porous Media 2(2011) 125.
12) B. K. Jha and H. M. Jibril: J. Phys. Soc. Jpn. 81 (2012) 024401.
13) V. P. Agrawal, N. K. Agrawal, and J. Singh: Int. J. Adv. Sci. Technol.Res. 1 (2011) 2249.

Power System Technology
ISSN:1000-3673

Received: 16-04-2025 Revised: 05-05-2025 Accepted: 22-07-2025

14) I. Khan, K. Fakhar, and S. Sharidan: Trans. Porous Media 91 (2012)49.
15) M. Navier: Mem. Acad. Sci. Inst. France 6 (1823) 389.
16) T. Hayat, S. Najam, and C. M. Khalique: J. Porous Media 13 (2010)999.
17) T. Hayat, S. Najam, and S. Asghar: J. Porous Media 13 (2010) 839.
18) A. Farhad, M. Norzieha, S. Sharidan, and I. Khan: Eur. J. Sci. Res. 57(2011) 293.
19) A. M. Siddiqui, T. Haroon, M. Zahid, and A. Shahzad: World Appl.Sci. J. 13 (2011) 2282.
20) N. K. Verma, S. Mishra, S. U. Siddiqui, and R. S. Gupta: Appl. Math.2 (2011) 764.
21) T. Hayat, M. Qasim, and S. Mesloub: Int. J. Numer. Methods Fluids 66(2011) 963.
22) M. Qasim, T. Hayat, and A. A. Hendi: Heat Trans. Asian Res. 40(2011) 641.
23) O. D. Makinde and P. Y. Mhone: Rom. J. Phys. 50 (2005) 931.
24) A. Mehmood and A. Ali: Rom. J. Phys. 52 (2007) 85.
25) A. Kumar, C. L. Varshney, and S. Lal: J. Eng. Technol. Res. 2 (2010)73.
26) B. K. Jha and C. A. Apere: J. Phys. Soc. Jpn. 79 (2010) 104401.
27) I. Khan, F. Ali, S. Sharidan, and M. Norzieha: J. Phys. Soc. Jpn. 80(2011) 064401.
28) I. Khan, K. Fakhar, and S. Sharidan: J. Phys. Soc. Jpn. 80 (2011)104401.
29) A. C. L. Cogley, W. G. Vinvent, and E. S. Giles: AIAA paper 551(1968)